
Contrastive Learning Is Spectral Clustering On Similarity Graph

Zhiqian Tan*

Department of Math, Tsinghua University
tanzq21@mails.tsinghua.edu.cn

Yifan Zhang*

IIIS, Tsinghua University
zhangyif21@mails.tsinghua.edu.cn

Jingqin Yang*

IIIS, Tsinghua University
yangjq21@mails.tsinghua.edu.cn

Yang Yuan†

IIIS, Tsinghua University
Shanghai Artificial Intelligence Laboratory
Shanghai Qi Zhi Institute
yuanyang@tsinghua.edu.cn

Abstract

Contrastive learning is a powerful self-supervised learning method, but we have a limited theoretical understanding of how it works and why it works. In this paper, we prove that contrastive learning with the standard InfoNCE loss is equivalent to spectral clustering on the similarity graph. Using this equivalence as the building block, we extend our analysis to the CLIP model and rigorously characterize how similar multi-modal objects are embedded together. Motivated by our theoretical insights, we introduce the kernel mixture loss, incorporating novel kernel functions that outperform the standard Gaussian kernel on several vision datasets.

1 Introduction

Contrastive learning is one of the most popular self-supervised learning methods, particularly for vision tasks (Chen et al., 2020a; He et al., 2019). It trains a neural network to map a collection of objects into an embedding space, ensuring that similar objects are in close proximity while dissimilar objects remain distant. A widely used loss function utilized to accomplish this objective is the InfoNCE loss, as exemplified by SimCLR (Chen et al., 2020a).

In the inspiring work, HaoChen et al. (2021) showed that if one replaces the standard InfoNCE loss with their spectral contrastive loss, contrastive learning is doing spectral clustering on the population augmentation graph. However, the spectral contrastive loss is rarely used empirically, and cannot be used for analyzing the performance of various similarity functions in the embedding space. Moreover, using the spectral contrastive loss, the final embedding is a combination of the standard spectral clustering and an additional linear transformation. Thus, the existing results cannot connect the original InfoNCE loss with the standard spectral clustering.

In this paper, we prove that SimCLR, the standard contrastive learning method, performs spectral clustering without modifying the InfoNCE loss or applying additional transformations to the embeddings. Our analysis with a collection of n objects $\mathbf{X} = [\mathbf{X}_1, \dots, \mathbf{X}_n]$ in space \mathcal{X} . For these objects, we define a similarity graph with adjacency matrix π , such that $\pi_{i,j}$ equals the probability of \mathbf{X}_i and \mathbf{X}_j being paired together in the data augmentation step of contrastive learning.

*Equal Contribution

†Corresponding Author

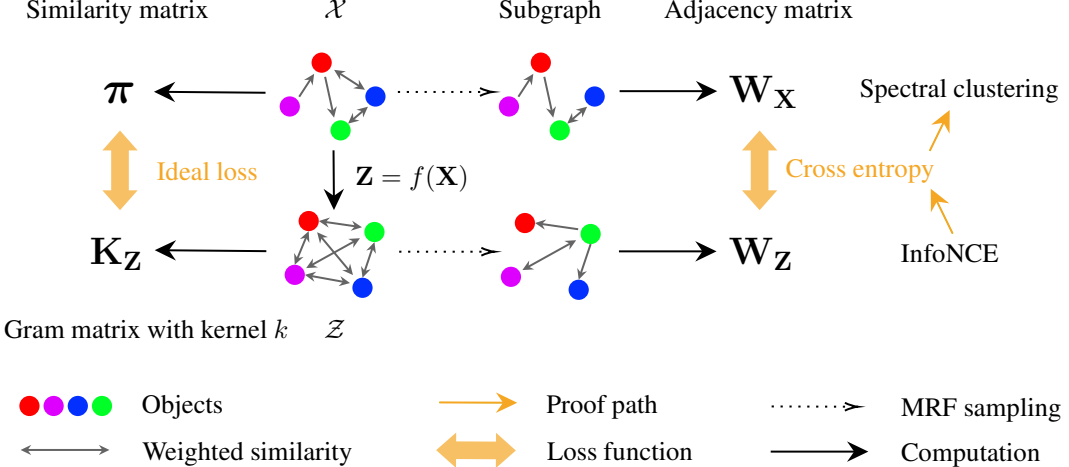


Figure 1: An illustration of our analysis.

Given this similarity graph, we want to find an embedding function $f : \mathcal{X} \rightarrow \mathcal{Z}$. Denote $\mathbf{Z} \triangleq f(\mathbf{X})$ as the embedding of \mathbf{X} , and our objective is to ensure that the gram matrix \mathbf{K}_Z with kernel k representing the similarities for \mathbf{Z} is as close to π as possible. See Figure 1 for an illustration.

However, directly comparing π with \mathbf{K}_Z can be difficult, as there are too many edges in both graphs. Therefore, we define two Markov random fields (MRFs) based on π and \mathbf{K}_Z , and compare the MRFs instead. Indeed, each MRF introduces a probability distribution of unweighted directed subgraphs on n objects (Van Assel et al., 2022), denoted as \mathbf{W}_X and \mathbf{W}_Z respectively. As a natural approximation to the ideal loss between π and \mathbf{K}_Z , we use the cross entropy loss between \mathbf{W}_X and \mathbf{W}_Z . The surprising discovery of our paper is that the InfoNCE loss is equivalent to the cross entropy loss when each subgraph is restricted to have an out-degree of exactly one. Moreover, when k is the Gaussian kernel, optimizing the cross entropy loss is equivalent to running spectral clustering on π . Combining the two observations, we conclude that using the InfoNCE loss is equivalent to running spectral clustering.

Our characterization of contrastive learning depends on two key factors: the augmentation step that defines a similarity graph, and the InfoNCE loss that measures the distance between two MRFs. Therefore, any other models with these two factors can be analyzed similarly. In particular, the CLIP (Radford et al., 2021) model for multi-modal learning belongs to this paradigm. Using the same framework, we prove a representation theorem for CLIP, showing that it runs spectral clustering on the bipartite graph induced by the paired training data.

Is it possible to improve the InfoNCE loss by using a different kernel? Based on the maximum entropy principle, we demonstrate that the exponential kernels are the natural choices for capturing the local similarity structure for contrastive learning. Moreover, they are also good candidates in terms of expressive power. Empirically, we observe that taking the mixture of Gaussian and Laplacian kernels, which maintain the aforementioned properties, can achieve better performance than the Gaussian kernel on several benchmark vision datasets.

In summary, our main contributions include:

- We prove the equivalence of SimCLR and spectral clustering on the similarity graph.
- We extend our analysis to the multi-modal setting and prove the equivalence of CLIP and spectral clustering on the multi-modal similarity graph.
- Inspired by theory, we propose new kernels that achieve better performance than the standard kernel empirically on the benchmark vision datasets.

2 Related Work

Contrastive learning is a classical method that was widely used in representation learning (Hadsell et al., 2006; Becker & Hinton, 1992). Since its recent applications in self-supervised learning, it has received prevalent attention and achieved state-of-the-art results on many downstream tasks in computer vision (Tian et al., 2020; Cui et al., 2021), graph representation learning (You et al., 2020; Hassani & Khasahmadi, 2020), multi-modality (Radford et al., 2021) and so on.

Contrastive predictive coding (Oord et al., 2018) is one of the first methods to apply the idea of contrastive learning in self-supervised learning. After that, various methods seek to improve the performance. SimCLR (Chen et al., 2020a) and MoCo (Chen et al., 2020b) propose to use a large batch size and momentum update mechanism to ensure the effectiveness of learning. To alleviate the influence of false negative sampling, the hard negative sampling method (Kalantidis et al., 2020) has also been discussed.

Although contrastive learning has reached empirical success, the theoretical understanding of its mechanism is still limited. Oord et al. (2018) show that InfoNCE loss can be seen as a surrogate loss for maximizing the mutual information. HaoChen et al. (2021) introduce the concept of augmentation graph to help analyze contrastive learning. Hu et al. (2022) connect contrastive learning with stochastic neighbor embedding. Wang & Isola (2020) show that the quality of embedding may decompose into an alignment part and a uniformity part, by taking both the loss function and the embedding space into consideration.

3 Background

In this paper, we use objects to denote data points like images or texts. Given a matrix \mathbf{X} , we use \mathbf{X}_i to denote its i -th row, and $\mathbf{X}_{i,j}$ to denote its (i, j) -th entry. Same holds for matrices like $\mathbf{W}_\mathbf{X}$, where we use $\mathbf{W}_{\mathbf{X},i}$ and $\mathbf{W}_{\mathbf{X},i,j}$, respectively.

3.1 Contrastive learning: SimCLR

Given a query object $\mathbf{q} \in \mathcal{X}$, one similar object \mathbf{p}_1 for \mathbf{q} , and $N - 1$ other objects $\{\mathbf{p}_i\}_{i=2}^N$, SimCLR finds a function f (usually a neural network) that maps these objects to \mathcal{Z} , to minimize the InfoNCE loss of \mathbf{q} :

$$\mathcal{L}(\mathbf{q}, \mathbf{p}_1, \{\mathbf{p}_i\}_{i=2}^N) = -\log \frac{\exp(\text{sim}(f(\mathbf{q}), f(\mathbf{p}_1))/\tau)}{\sum_{i=1}^N \exp(\text{sim}(f(\mathbf{q}), f(\mathbf{p}_i))/\tau)} \quad (1)$$

Here, the actual loss of f takes the summation over different \mathbf{q} , and τ is a temperature hyperparameter. The $\text{sim}(\mathbf{Z}_i, \mathbf{Z}_j)$ function measures the similarity between $\mathbf{Z}_i, \mathbf{Z}_j$ in \mathcal{Z} , and is commonly defined as $\text{sim}(\mathbf{Z}_i, \mathbf{Z}_j) = \frac{\mathbf{Z}_i^\top \mathbf{Z}_j}{\|\mathbf{Z}_i\| \|\mathbf{Z}_j\|}$, or $\mathbf{Z}_i^\top \mathbf{Z}_j$, or $-\|\mathbf{Z}_i - \mathbf{Z}_j\|^2/2$. In this paper, we consider the case that \mathcal{Z} is the unit sphere, i.e., $\|\mathbf{Z}_i\| = \|\mathbf{Z}_j\| = 1$. This is because both SimCLR and CLIP have a normalization step in the implementation (Chen et al., 2020a; Radford et al., 2021). Hence,

$$\frac{\mathbf{Z}_i^\top \mathbf{Z}_j}{\|\mathbf{Z}_i\| \|\mathbf{Z}_j\|} = \mathbf{Z}_i^\top \mathbf{Z}_j, \text{ and}$$

$$-\|\mathbf{Z}_i - \mathbf{Z}_j\|^2/2 = -\mathbf{Z}_i^2/2 - \mathbf{Z}_j^2/2 + \mathbf{Z}_i^\top \mathbf{Z}_j = -1 + \mathbf{Z}_i^\top \mathbf{Z}_j. \quad (2)$$

Therefore, these losses are the same up to a constant.

3.2 Multi-modal learning: CLIP

CLIP (Radford et al., 2021) is a multi-modal model with a dataset containing millions of (image, text) pairs. During pretraining, for each batch of N pairs of data points, CLIP uses an image encoder and a text encoder to get N pairs of embeddings, and use the InfoNCE loss to compute the correct N pairs out of $N \times N$ possible connections. Specifically, given an image \mathbf{a}_i , we compare the its matching score of the paired text \mathbf{b}_i , with the matching scores of other $N - 1$ texts $\{\mathbf{b}_j\}_{j \neq i}$, using the loss $\ell(\mathbf{a}_i, \mathbf{b}_i, \{\mathbf{b}_j\}_{j \neq i})$ defined in Eqn. (1) by setting $\text{sim}(\mathbf{Z}_i, \mathbf{Z}_j) = \frac{\mathbf{Z}_i^\top \mathbf{Z}_j}{\|\mathbf{Z}_i\| \|\mathbf{Z}_j\|}$.

One can define the loss similarly for text, and the actual loss of the embedding network f takes the summation over all the images and texts.

3.3 Reproducing Kernel Hilbert Space

Given two objects $\mathbf{Z}_i, \mathbf{Z}_j \in \mathcal{Z}$, consider a feature map $\phi : \mathcal{Z} \rightarrow \mathcal{H}$, where the feature space \mathcal{H} is usually much larger than \mathcal{Z} . We may define a kernel k that measures the similarity of $\mathbf{Z}_i, \mathbf{Z}_j$ as $k(\mathbf{Z}_i, \mathbf{Z}_j) \triangleq \langle \phi(\mathbf{Z}_i), \phi(\mathbf{Z}_j) \rangle_{\mathcal{H}}$, i.e., the inner product between the two objects after mapping them to the feature space. For any vector $h \in \mathcal{H}$, it also corresponds to a function $h(\cdot) : \mathcal{Z} \rightarrow \mathbb{R}$, defined as $h(\mathbf{Z}_i) = \langle h, \phi(\mathbf{Z}_i) \rangle_{\mathcal{H}}$. Specifically, $\phi(\mathbf{Z}_j)$ as a vector in \mathcal{H} represents the function $k(\cdot, \mathbf{Z}_j) : \mathcal{Z} \rightarrow \mathbb{R}$, because for any $\mathbf{Z}_i \in \mathcal{Z}$, we have $k(\mathbf{Z}_i, \mathbf{Z}_j) = \langle \phi(\mathbf{Z}_i), \phi(\mathbf{Z}_j) \rangle_{\mathcal{H}}$. Formally, we have:

Definition 3.1 (Reproducing kernel Hilbert space). Let \mathcal{H} be a Hilbert space of \mathbb{R} -valued functions defined on a non-empty set \mathcal{Z} . A function $k : \mathcal{Z} \times \mathcal{Z} \rightarrow \mathbb{R}$ is called a reproducing kernel of \mathcal{H} , and \mathcal{H} is a reproducing kernel Hilbert space, if k satisfies

- $\forall \mathbf{Z}_i \in \mathcal{Z}, k(\cdot, \mathbf{Z}_i) \in \mathcal{H}$
- $\forall \mathbf{Z}_i \in \mathcal{Z}, \forall h \in \mathcal{H}, \langle h, k(\cdot, \mathbf{Z}_i) \rangle_{\mathcal{H}} = h(\mathbf{Z}_i)$.

We focus on the translation-invariant kernel in our paper, where the kernel $k(\mathbf{Z}_i, \mathbf{Z}_j)$ can always be written as $k'(\mathbf{Z}_i - \mathbf{Z}_j)$ for $k' \in \mathcal{Z} \rightarrow \mathbb{R}$. The Moore–Aronszajn’s theorem states that if k is a symmetric, positive definite kernel on \mathcal{Z} , there is a unique Hilbert space of functions \mathcal{H} on \mathcal{Z} for which k is a reproducing kernel.

For instance, the Gaussian kernel is a symmetric, positive definite kernel that yields an RKHS with infinite dimensions. One of the advantages of a reproducing kernel is that the similarity can be computed directly in \mathcal{Z} without using the feature map to go to the potentially infinite dimensional Hilbert space. However, a reproducing kernel’s similarity structure should ideally align with the semantic meanings of specific tasks. For example, it is unlikely to calculate the semantic similarity of two images directly using a predefined reproducing kernel in the pixel space.

Consequently, we ask if it is possible to find an embedding function $f : \mathcal{X} \rightarrow \mathcal{Z}$, where \mathcal{Z} can compute the similarity of two objects in \mathcal{X} with a predefined kernel function, i.e., whether $\mathbf{K}_{\mathbf{Z}}$ matches with $\boldsymbol{\pi}$ in Figure 1. In other words, we hope to map the objects to a space where the semantic similarity in \mathcal{X} is naturally embedded. This is the starting point of our paper.

3.4 Markov random field

In this subsection, we present the framework (without proofs) of MRF for dimension reduction (Van Assel et al., 2022). We have modified some definitions and lemmas for our learning scenarios, and the readers may check the paper for more details on this framework.

Consider n objects $\mathbf{Z} = [\mathbf{Z}_1, \dots, \mathbf{Z}_n]$ in \mathcal{Z} . We use a symmetric and translation invariant kernel $k : \mathcal{Z} \rightarrow \mathbb{R}_+$ to represent the similarities in \mathcal{Z} , where symmetric means $k(\mathbf{x}) = k(-\mathbf{x})$. Given \mathbf{Z} and k , we define the gram matrix as $\mathbf{K}_{\mathbf{Z}} \triangleq (k(\mathbf{Z}_i - \mathbf{Z}_j))_{(i,j) \in [n]^2}$, which is also the adjacency matrix representing the similarities of objects in \mathbf{Z} .

As discussed previously, directly comparing $\mathbf{K}_{\mathbf{Z}}$ and $\boldsymbol{\pi}$ can be difficult, so we treat them as MRFs and compare the induced probability distributions on subgraphs instead. In our paper, subgraphs are directed unweighted graphs from the set $S_{\mathbf{W}} \triangleq \{\mathbf{W} \in \{0, 1\}^{n \times n} \mid \forall (i, j) \in [n]^2, \mathbf{W}_{i,i} = 0\}$. The distribution of \mathbf{W} is generally defined as follows.

Definition 3.2 (Distribution of \mathbf{W}). Let $\boldsymbol{\pi} \in \mathbb{R}_+^{n \times n}$, we define the distribution $\mathbb{P}(\mathbf{W}; \boldsymbol{\pi}) \propto \Omega(\mathbf{W}) \prod_{(i,j) \in [n]^2} \boldsymbol{\pi}_{i,j}^{\mathbf{W}_{i,j}}$, where $\Omega(\mathbf{W}) \triangleq \prod_i \mathbb{I}_{\sum_j \mathbf{W}_{i,j}=1}$.

To provide a clearer interpretation of the definition, we can break down the expression $\Omega(\mathbf{W}) \prod_{(i,j) \in [n]^2} \boldsymbol{\pi}_{i,j}^{\mathbf{W}_{i,j}}$ into two parts. Firstly, $\Omega(\mathbf{W})$ checks if each row i of \mathbf{W} has exactly one out-going edge. Therefore, only subgraphs with a unitary out-degree will be preserved, while subgraphs with other out-degree values will be filtered out. As we will see later, this exactly corresponds to the setting that the InfoNCE loss uses exactly one positive neighbor. Secondly, $\prod_{(i,j) \in [n]^2} \boldsymbol{\pi}_{i,j}^{\mathbf{W}_{i,j}}$ multiplies the scores of each edge in $\boldsymbol{\pi}$ compared with $\mathbf{W}_{i,j}$. This multiplication results in the unnormalized likelihood of \mathbf{W} under $\boldsymbol{\pi}$. See Figure 2 for an illustration.

By applying Definition 3.2 to $\mathbf{K}_{\mathbf{Z}}$, we obtain the following expression for $\mathbb{P}(\mathbf{W}; \mathbf{K}_{\mathbf{Z}})$: $\mathbb{P}(\mathbf{W}; \mathbf{K}_{\mathbf{Z}}) \propto \Omega(\mathbf{W}) \prod_{(i,j) \in [n]^2} k(\mathbf{Z}_i - \mathbf{Z}_j)^{\mathbf{W}_{i,j}}$. This expression represents the prior probability of \mathbf{W} under $\mathbf{K}_{\mathbf{Z}}$.

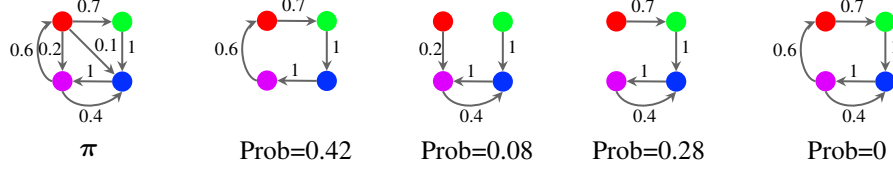


Figure 2: Sampling probabilities of the subgraphs defined by $\mathbb{P}(\mathbf{W}; \boldsymbol{\pi})$. The first subfigure represents the underlying graph $\boldsymbol{\pi}$, the next three subfigures represent three different subgraphs with their sampling probabilities. The last subfigure has sampling probability 0 because the purple node has out-degree larger than 1.

Due to the unitary out-degree filter, $\mathbb{P}(\mathbf{W}; \boldsymbol{\pi})$ has the following property.

Lemma 3.3. For $\mathbf{W} \sim \mathbb{P}(\cdot; \boldsymbol{\pi})$, $\forall i \in [n]$, $\mathbf{W}_i \sim \mathcal{M}(1, \boldsymbol{\pi}_i / \sum_j \boldsymbol{\pi}_{i,j})$, where \mathcal{M} is the multinomial distribution. Moreover, given any $i, i' \in [n]$, \mathbf{W}_i is independent to $\mathbf{W}_{i'}$. Where \mathbf{W}_i is the i -th row of \mathbf{W} , $\boldsymbol{\pi}_i$ is the i -th row of $\boldsymbol{\pi}$.

Below we define the cross entropy loss given distribution $\boldsymbol{\pi}$ and the similarity matrix \mathbf{K}_Z .

$$\mathcal{H}_{\boldsymbol{\pi}}^k(\mathbf{Z}) \triangleq -\mathbb{E}_{\mathbf{W}_Z \sim \mathbb{P}(\cdot; \boldsymbol{\pi})} [\log \mathbb{P}(\mathbf{W}_Z = \mathbf{W}_Z; \mathbf{K}_Z)] \quad (3)$$

The following lemma will be helpful in analyzing the cross-entropy loss, which states that when the two distributions can be aligned and decomposed, their cross entropy loss can also be decomposed.

Lemma 3.4. Assume $\mathcal{X} = \mathcal{X}_1 \times \cdots \times \mathcal{X}_k$ and there are two probability distributions \mathbf{P} and \mathbf{Q} supported on \mathcal{X} . Suppose $\mathbf{P} = \mathbf{P}_1 \otimes \cdots \otimes \mathbf{P}_k$ and $\mathbf{Q} = \mathbf{Q}_1 \otimes \cdots \otimes \mathbf{Q}_k$, with \mathbf{P}_i and \mathbf{Q}_i supported on \mathcal{X}_i . Let $\mathcal{H}(\mathbf{P}, \mathbf{Q}) \triangleq -\mathbb{E}_{x \sim \mathbf{P}} [\log \mathbf{Q}(x)]$. Then $\mathcal{H}(\mathbf{P}, \mathbf{Q}) = \sum_{i=1}^k \mathcal{H}(\mathbf{P}_i, \mathbf{Q}_i)$.

The cross-entropy loss can be converted to the combination of repulsion and attraction terms.

Lemma 3.5. $\min_{\mathbf{Z}} \mathcal{H}_{\boldsymbol{\pi}}^k(\mathbf{Z})$ is equivalent to

$$\min_{\mathbf{Z}} - \sum_{(i,j) \in [n]^2} \mathbf{P}_{i,j} \log k(\mathbf{Z}_i - \mathbf{Z}_j) + \log \mathbf{R}(\mathbf{Z}), \quad (4)$$

where $\mathbf{P} = \mathbb{E}_{\mathbf{W}_Z \sim \mathbb{P}(\cdot; \boldsymbol{\pi})} [\mathbf{W}_Z]$, and $\mathbf{R}(\mathbf{Z}) = \sum_{\mathbf{W} \in S_{\mathbf{W}}} \mathbb{P}(\mathbf{Z}, \mathbf{W})$ with $\mathbb{P}(\mathbf{Z}, \mathbf{W}) \propto f_k(\mathbf{Z}, \mathbf{W}) \Omega(\mathbf{W})$.

The second term in Eqn. (4) punishes trivial solutions like $\mathbf{Z} = \mathbf{0}$, as $\mathbf{0}$ is a mode for $f_k(\cdot, \mathbf{W})$ for any \mathbf{W} , which incurs large $\log \mathbf{R}(\mathbf{Z})$. The first term can be interpreted using the graph Laplacian operator, defined below.

Definition 3.6 (Graph Laplacian operator). The graph Laplacian operator is a function \mathbf{L} that maps a $n \times n$ nonnegative matrix to a positive semidefinite matrix such that:

$$\forall i, j \in [n]^2, \mathbf{L}(\mathbf{W})_{i,j} = \begin{cases} -\mathbf{W}_{i,j} & \text{if } i \neq j \\ \sum_{k \in [n]} \mathbf{W}_{i,k} & \text{o.w.} \end{cases}$$

By simple calculation, when k is the Gaussian kernel, the first term in Eqn. (4) becomes $\text{tr}(\mathbf{Z}^T \mathbf{L}^* \mathbf{Z})$ where $\mathbf{L}^* = \mathbb{E}_{\mathbf{W}_Z \sim \mathbb{P}(\cdot; \boldsymbol{\pi})} [\mathbf{L}(\mathbf{W}_Z)]$. In other words, Eqn. (4) is equivalent to doing spectral clustering with a repulsion regularizer $\log \mathbf{R}(\mathbf{Z})$.

4 Contrastive Learning: SimCLR

We assume that there are finitely many objects in \mathcal{X} , denoted as n . This is the same assumption used by HaoChen et al. (2021), who also demonstrated that the finite case can be easily extended to the infinite case by replacing sum by integral, adjacency matrix by adjacency operator, etc. For continuous augmentation methods like adding Gaussian noise, we can discretize it in a natural way. Assuming a finite number of objects can help us avoid non-essential technical jargon.

With n objects in \mathcal{X} , consider a similarity graph defined on these objects, which gives a similarity matrix π of size $n \times n$. However, for real scenarios like learning images, it is extremely difficult to obtain such π from human labeling. Therefore, we compute π using the prior knowledge of the dataset. For example, in the original SimCLR paper (Chen et al., 2020a), there are 9 different augmentation methods. Each augmentation method may generate many different augmented images that look similar to the original image. For every original image \mathbf{X}_i , we define a probability distribution π_i , such that each object \mathbf{X}_j gets sampled with probability $\pi_{i,j}$. Therefore, π_i can be represented as a vector in \mathbb{R}_+^n .

Stacking all probability distributions π_i together for $i \in [n]$, we get a matrix $\pi \in \mathbb{R}_+^{n \times n}$. We assume the sampling process is symmetric, i.e., $\pi_{i,j} = \pi_{j,i}$. The stochastic data augmentation samples \mathbf{W}_X based on π , i.e., $\mathbf{W}_X \sim \mathbb{P}(\cdot; \pi)$.

4.1 Main Theorem

Theorem 4.1. *For the SimCLR algorithm, denote f as the neural network, $\mathbf{Z} \triangleq f(\mathbf{X})$, and π as the similarity graph defined by the data augmentation process. Then SimCLR is equivalent to solving the following program:*

$$\min_{\mathbf{Z}} \text{tr}(\mathbf{Z}^\top \mathbf{L}(\pi) \mathbf{Z}) + \log \mathbf{R}(\mathbf{Z})$$

which runs spectral clustering on π .

Proof. Our proof has two steps. In Step 1, we will show that SimCLR is equivalent to minimizing the cross entropy loss defined in Eqn. (3). In Step 2, we will show that minimizing the cross entropy loss is equivalent to spectral clustering on π . Combining the two steps together, we have proved our theorem.

Step 1: SimCLR is equivalent to minimizing the cross entropy loss.

The cross entropy loss takes expectation over $\mathbf{W}_X \sim \mathbb{P}(\cdot; \pi)$, which means \mathbf{W}_X has exactly one non-zero entry in each row i . By Lemma 3.3, we know every row i of \mathbf{W}_X is independent of other rows. Moreover, $\mathbf{W}_{X,i} \sim \mathcal{M}(1, \pi_i / \sum_j \pi_{i,j}) = \mathcal{M}(1, \pi_i)$, because π_i itself is a probability distribution. Similarly, we know \mathbf{W}_Z also has the row-independent property by sampling over $\mathbb{P}(\cdot; \mathbf{K}_Z)$. Therefore, by Lemma 3.4, we know Eqn. (3) is equivalent to:

$$-\sum_{i=1}^n \mathbb{E}_{\mathbf{W}_{X,i}} [\log \mathbb{P}(\mathbf{W}_{Z,i} = \mathbf{W}_{X,i}; \mathbf{K}_Z)]$$

This expression takes expectation over $\mathbf{W}_{X,i}$ for the given row i . Notice that $\mathbf{W}_{X,i}$ has exactly one non-zero entry, which equals 1 (same for $\mathbf{W}_{Z,i}$). As a result we expand the above expression to be:

$$-\sum_{i=1}^n \sum_{j \neq i} \Pr(\mathbf{W}_{X,i,j} = 1) \log \Pr(\mathbf{W}_{Z,i,j} = 1) \tag{5}$$

By Lemma 3.3, $\Pr(\mathbf{W}_{Z,i,j} = 1) = \mathbf{K}_{Z,i,j} / \|\mathbf{K}_{Z,i}\|_1$ for $j \neq i$. Recall that $\mathbf{K}_Z = (k(\mathbf{Z}_i - \mathbf{Z}_j))_{(i,j) \in [n]^2}$, which means $\mathbf{K}_{Z,i,j} / \|\mathbf{K}_{Z,i}\|_1 = \frac{\exp(-\|\mathbf{Z}_i - \mathbf{Z}_j\|^2/2\tau)}{\sum_{k \neq i} \exp(-\|\mathbf{Z}_i - \mathbf{Z}_k\|^2/2\tau)}$ for $j \neq i$, when k is the Gaussian kernel with variance τ .

Notice that $\mathbf{Z}_i = f(\mathbf{X}_i)$, so we know

$$-\log \Pr(\mathbf{W}_{Z,i,j} = 1) = -\log \frac{\exp(-\|f(\mathbf{X}_i) - f(\mathbf{X}_j)\|^2/2\tau)}{\sum_{k \neq i} \exp(-\|f(\mathbf{X}_i) - f(\mathbf{X}_k)\|^2/2\tau)} \tag{6}$$

The right hand side is exactly the InfoNCE loss defined in Eqn. (1). Inserting Eqn. (6) into Eqn. (5), we get the SimCLR algorithm, which first samples augmentation pairs (i, j) with $\Pr(\mathbf{W}_{X,i,j} = 1)$ for each row i , and then optimize the InfoNCE loss.

Step 2: minimizing the cross entropy loss is equivalent to spectral clustering on π .

By Lemma 3.5, we may further convert the loss to

$$\min_{\mathbf{Z}} - \sum_{(i,j) \in [n]^2} \mathbf{P}_{i,j} \log k(\mathbf{Z}_i - \mathbf{Z}_j) + \log \mathbf{R}(\mathbf{Z}) \quad (7)$$

Since k is the Gaussian kernel, this reduces to

$$\min_{\mathbf{Z}} \text{tr}(\mathbf{Z}^\top \mathbf{L}(\boldsymbol{\pi}) \mathbf{Z}) + \log \mathbf{R}(\mathbf{Z})$$

where we use the fact that $\mathbb{E}_{\mathbf{W}_X \sim \mathbb{P}(\cdot; \boldsymbol{\pi})} [\mathbf{L}(\mathbf{W}_X)] = \mathbf{L}(\boldsymbol{\pi})$, because the Laplacian operator is linear and $\mathbb{E}_{\mathbf{W}_X \sim \mathbb{P}(\cdot; \boldsymbol{\pi})} (\mathbf{W}_X) = \boldsymbol{\pi}$. \square

Discussions. Empirically, the InfoNCE loss is applied to a large batch of the object, rather than all the n objects that Theorem 4.1 requires. This explains why SimCLR benefits from larger batch size, e.g. Chen et al. (2020a) uses a batch size of 4096, and He et al. (2019) uses an even large memory bank for storing more samples.

While using the same framework from (Van Assel et al., 2022), our Theorem 4.1 is significantly different from their results on dimension reduction from at least two aspects. Firstly, in the object space \mathcal{X} , we have a predefined similarity graph $\boldsymbol{\pi}$, but they were using a kernel matrix \mathbf{K}_X based on \mathbf{X} and a kernel $k_{\mathcal{X}}$. This is because in the dimension reduction setting, the input objects are assumed to be well-structured data points, but in the self-supervised learning setting, the input objects are images or texts, where a translation invariant kernel cannot be used for computing the similarities. Secondly, their cross-entropy loss is directly computed from \mathbf{K}_X , while \mathbf{W}_X is never explicitly sampled. In contrast, in our method, $\boldsymbol{\pi}$ is never explicitly used, and the cross entropy loss is indirectly computed from the randomly sampled \mathbf{W}_X .

The equivalence we proved is exact. Therefore, after learning, the embedding space contains different components, corresponding to various (sub-) classes of the objects. This characterization naturally explains why contrastive learning works well for classification related downstream tasks.

5 Multi-modal Learning

5.1 Original CLIP

In this subsection, we extend Theorem 4.1 to the multi-modal setting by analyzing CLIP, which applies the contrastive loss to the image-text pairs. The image-text pairs can be represented with the following pair graph.

Definition 5.1 (Pair graph). Consider two modalities of objects \mathbf{A}, \mathbf{B} , and undirected unit-weight edges $\mathbf{E} = \{(\mathbf{a}_i, \mathbf{b}_i) \mid \mathbf{a}_i \in \mathbf{A}, \mathbf{b}_i \in \mathbf{B}\}_{i=1}^M$. The pair graph between \mathbf{A}, \mathbf{B} is a directed bipartite graph $\boldsymbol{\pi}_{\mathbf{A}, \mathbf{B}} = (\mathbf{A}, \mathbf{B}, \mathbf{E})$, with the weight of each outgoing edge normalized by the out-degree of the node.

By definition, $\boldsymbol{\pi}_{\mathbf{A}, \mathbf{B}}$ is not necessarily symmetric. Consider the case where the dataset contains 10 images of “dog”, all of them are connected to the same text “dog”. In this case, the text dog has 1/10 probability to each image, while each image has only one edge with 100% probability to the text. However, since each row of $\boldsymbol{\pi}_{\mathbf{A}, \mathbf{B}}$ is still a probability distribution, we still have the next theorem.

Theorem 5.2 (CLIP’s objective). *For the CLIP algorithm, denote $\boldsymbol{\pi}_{\mathbf{A}, \mathbf{B}}$ as the pair graph. Then CLIP is equivalent to running the generalized spectral clustering on $\boldsymbol{\pi}_{\mathbf{A}, \mathbf{B}}$.*

Proof. Since $\mathbf{W}_X \sim \mathbb{P}(\cdot; \boldsymbol{\pi}_{\mathbf{A}, \mathbf{B}})$, we know \mathbf{W}_X has exactly one non-zero entry in each row, denoting the pair got sampled. A notable difference compared to the previous proof, is we now have $n_{\mathcal{A}} + n_{\mathcal{B}}$ objects in our graph. CLIP deals with this by taking a mini-batch of size $2N$, such that $n_{\mathcal{A}} = n_{\mathcal{B}} = N$, and add the $2N$ InfoNCE losses together. We label the objects in \mathcal{A} as $[n_{\mathcal{A}}]$, and the objects in \mathcal{B} as $\{n_{\mathcal{A}} + 1, \dots, n_{\mathcal{A}} + n_{\mathcal{B}}\}$.

Notice that $\boldsymbol{\pi}_{\mathbf{A}, \mathbf{B}}$ is a bipartite graph, so the edges of objects in \mathcal{A} will only connect to object in \mathcal{B} and vice versa. We can define the similarity matrix in \mathcal{Z} as \mathbf{K}_Z , where $\mathbf{K}_Z(i, j + n_{\mathcal{A}}) = \mathbf{K}_Z(j + n_{\mathcal{A}}, i) = k(\mathbf{Z}_i - \mathbf{Z}_j)$ for $i \in [n_{\mathcal{A}}], j \in [n_{\mathcal{B}}]$, and otherwise we set $\mathbf{K}_Z(i, j) = 0$. The rest is same as the previous proof. \square

Discussions. In Theorem 5.2, we say CLIP runs the generalized spectral clustering because $\mathbf{L}(\pi_{\mathbf{A}, \mathbf{B}})$ is not necessarily the Laplacian of a symmetric graph, although one can still compute the optimal embedding \mathbf{Z} following Eqn. (4).

Theorem 5.2 also assumes that all the objects are sampled in $\mathbf{W}_{\mathbf{X}}$, while empirically a really big batch size of 32,768 is used in Radford et al. (2021). Moreover, the probability distribution $\mathbb{P}(\cdot; \pi_{\mathbf{A}, \mathbf{B}})$ used in Theorem 5.2 is slightly different from the implementation of CLIP, in the sense that CLIP uniformly samples the edges in \mathbf{E} , but here we uniformly sample the objects in $\mathbf{A} \cup \mathbf{B}$. When the image-text pairs dataset has high quality, the difference between these two sampling schemes becomes negligible as the variance of object out-degrees is extremely small.

However, the pair graph usually contains a huge number of isolated edges (thus isolated components), which means the outcome of spectral clustering is less interesting. Empirically, CLIP picks strong image and text encoders with good prior knowledge about the dataset. Such prior knowledge may bias towards a better embedding for grouping the isolated edges with more semantics. Inspired by Theorem 5.2, we also propose two augmented CLIP algorithms for better theoretical guarantees, see Appendix A.

6 With New Kernels

We have seen that the InfoNCE loss is equivalent to Eqn. (4) for various settings. Can we replace the Gaussian kernel in Eqn. (4) with new kernels for better performance? In this section, we examine InfoNCE-like losses with the maximum entropy principle and subsequently evaluate the expressive power of different kernel functions. Our analysis leads us to conclude that the exponential kernel is a promising candidate for replacing the Gaussian kernel. Specifically, we consider a mixture of Gaussian and Laplacian kernels as potential alternatives for experimentation purposes.

6.1 Maximum entropy principle

In this subsection, we provide an interpretation of InfoNCE-like loss, which indicates that exponential kernels are the natural choices for our setting. Given a contrastive sample \mathbf{q} , denote ψ_i as the similarity between the \mathbf{q} and the contrastive sample \mathbf{p}_i for $i \in [n]$, computed by a kernel k . WLOG, assume \mathbf{p}_1 is the neighbor of \mathbf{q} by the prior knowledge, but ψ_1 is not necessarily the largest one in $\{\psi_i\}$. Ideally, we hope ψ_1 is the largest, or at least among one of the few largest similarities, which indicates our kernel properly matches with the prior knowledge of \mathcal{X} .

To optimize towards this goal, we shall design a loss function to capture how ψ_1 ranks. Since the ordering function is discrete without gradient information, we have to convert it into a soft and continuous function that makes gradient based optimization possible. Specifically, we use a probability distribution $\boldsymbol{\alpha}$ to represent the neighborhood structure of \mathbf{q} related to ψ_1 , which satisfies $\psi_1 \leq \sum_{i=1}^n \alpha_i \psi_i$, and $\forall i, \alpha_i \geq 0$. If ψ_1 is the largest, $\boldsymbol{\alpha} = e_1$ is the only solution, otherwise $\boldsymbol{\alpha}$ can be more diverse. For example, when all ψ_i 's are equal to each other, $\boldsymbol{\alpha}$ can be the uniform distribution.

Intuitively, if there are many other ψ_i 's with similar values as ψ_1 , the neighborhood structure of \mathbf{q} is not as good as ψ_1 being the only close object to \mathbf{q} . Formally, it means $\boldsymbol{\alpha}$ should have fewer non-zero entries, or at least concentrate at α_1 . We use its entropy $H(\boldsymbol{\alpha}) = -\sum_{i=1}^n \alpha_i \log \alpha_i$ to represent this diversity, which gives the following optimization problem.

$$(P1) \quad \begin{aligned} & \max_{\boldsymbol{\alpha}} && H(\boldsymbol{\alpha}) \\ & \text{s.t.} && \boldsymbol{\alpha}^\top \mathbf{1}_n = 1, \alpha_1, \dots, \alpha_n \geq 0 \\ & && \psi_1 - \sum_{i=1}^n \alpha_i \psi_i \leq 0 \end{aligned}$$

By minimizing the solution of (P1), we can find an embedding that better approximates the prior knowledge. However, how can we solve (P1)? By introducing the Lagrangian dual variable $\tau > 0$, we get the following program (P2) that generates an upper bound of (P1). As a result, minimizing (P2) simultaneously generates a smaller upper bound of (P1) as well, which helps us achieve our goal indirectly.

$$(P2) \quad \begin{aligned} & \max_{\boldsymbol{\alpha}} && -E(\boldsymbol{\alpha}) \\ & \text{s.t.} && \boldsymbol{\alpha}^\top \mathbf{1}_n = 1, \alpha_1, \dots, \alpha_n \geq 0 \end{aligned}$$

where $E(\boldsymbol{\alpha}) = \psi_1 - \sum_{i=1}^n \alpha_i \psi_i + \tau \sum_{i=1}^n \alpha_i \log \alpha_i$.

We have the following theorem for solving (P2).

Theorem 6.1 (Exponential kernels are natural). *The solution of (P2) satisfies:*

$$-E(\boldsymbol{\alpha}^*) = -\tau \log \frac{\exp(\frac{1}{\tau}\psi_1)}{\sum_{i=1}^n \exp(\frac{1}{\tau}\psi_i)}.$$

Proof. Because the objective function is a linear term adding an entropy regularization, which is a strongly concave function, the maximization problem is a convex optimization problem. Thanks to the implicit constraints given by the entropy function, the problem is equivalent to having only the equality constraint. We shall then introduce the Lagrangian multiplier λ and get the following relaxed problem:

$$\tilde{E}(\boldsymbol{\alpha}) = \psi_1 - \sum_{i=1}^n \alpha_i \psi_i + \tau \sum_{i=1}^n \alpha_i \log \alpha_i + \lambda (\boldsymbol{\alpha}^\top \mathbf{1}_n - 1).$$

As the relaxed problem is an unconstrained problem, taking the derivative with respect to α_i , we shall get

$$\frac{\partial \tilde{E}(\boldsymbol{\alpha})}{\partial \alpha_i} = -\psi_i + \tau \left(\log \alpha_i + \alpha_i \frac{1}{\alpha_i} \right) + \lambda = 0.$$

Solving the above equation implies that α_i has the form $\alpha_i = \exp(\frac{1}{\tau}\psi_i) \exp(\frac{-\lambda}{\tau} - 1)$. As α_i lying on the probability simplex, the optimal α_i is explicitly given by $\alpha_i^* = \frac{\exp(\frac{1}{\tau}\psi_i)}{\sum_{i'=1}^n \exp(\frac{1}{\tau}\psi_{i'})}$. Substituting the optimal point into the objective function, we have

$$\begin{aligned} E(\boldsymbol{\alpha}^*) &= \psi_1 - \sum_{i=1}^n \frac{\exp(\frac{1}{\tau}\psi_i)}{\sum_{i'=1}^n \exp(\frac{1}{\tau}\psi_{i'})} \psi_i + \tau \sum_{i=1}^n \frac{\exp(\frac{1}{\tau}\psi_i)}{\sum_{i'=1}^n \exp(\frac{1}{\tau}\psi_{i'})} \log \frac{\exp(\frac{1}{\tau}\psi_i)}{\sum_{i'=1}^n \exp(\frac{1}{\tau}\psi_{i'})} \\ &= \psi_1 - \tau \log \left(\sum_{i=1}^n \exp\left(\frac{1}{\tau}\psi_i\right) \right). \end{aligned}$$

Thus, the Lagrangian dual function is given by

$$-E(\boldsymbol{\alpha}^*) = -\tau \log \frac{\exp(\frac{1}{\tau}\psi_1)}{\sum_{i=1}^n \exp(\frac{1}{\tau}\psi_i)}.$$

□

With this framework, we can derive results similar to Tian (2022)'s max-min optimization formulation as a corollary.

Theorem 6.1 indicates that the loss function of the form $-\tau \log \frac{\exp(\frac{1}{\tau}\psi_1)}{\sum_{i=1}^n \exp(\frac{1}{\tau}\psi_i)}$ is a natural choice for characterizing the neighborhood similarity structure. In other words, we should use the exponential kernels defined as follows.

$$K_{\text{exp}}^{\gamma, \sigma}(x, y) \triangleq \exp\left(-\frac{\|x - y\|^\gamma}{\sigma}\right) \quad (\gamma, \sigma > 0) \quad (8)$$

We define our kernel-based contrastive loss Kernel-InfoNCE as below:

$$\mathcal{L}_{\text{Kernel-InfoNCE}}^{\gamma, \sigma}(\mathbf{q}, \mathbf{p}_1, \{\mathbf{p}_i\}_{i=2}^N) \triangleq -\log \frac{K_{\text{exp}}^{\gamma, \sigma}(\mathbf{q}, \mathbf{p}_1)}{\sum_{i=1}^N K_{\text{exp}}^{\gamma, \sigma}(\mathbf{q}, \mathbf{p}_i)} \quad (9)$$

Below we further investigate the kernels from expressive power and kernel mixture.

6.2 Expressive power

Based on Definition 3.1, we know the size of \mathcal{H} depends on how k is defined. For different exponential kernels, which one is more expressive? Specifically, can we find another kernel k' so that $\mathcal{H}_{k'}$ is larger than $\mathcal{H}_{\text{Gauss}}$? The answer is affirmative by the following Theorem.

Theorem 6.2 (Chen & Xu (2020)). *Consider exponential kernels restricted to the unit sphere \mathbb{S}^{d-1} and defined on the entire \mathbb{R}^d , respectively. Then we have the following RKHS inclusions: If $0 < \gamma \leq 1$, for any $\sigma > 0$, $\mathcal{H}_{\text{Gauss}}(\mathbb{S}^{d-1}) \subseteq \mathcal{H}_{K_{\text{exp}}^{\gamma, \sigma}}(\mathbb{S}^{d-1})$ and $\mathcal{H}_{\text{Gauss}}(\mathbb{R}^d) \subseteq \mathcal{H}_{K_{\text{exp}}^{\gamma, \sigma}}(\mathbb{R}^d)$.*

This implies, at least from the perspective of expressive power, picking a smaller number on the exponential is better. Note that when $\gamma = 1$, we get the Laplacian kernel.

6.3 Kernel Mixture

In the previous subsections, we have seen that exponential kernels have many attractive properties. In this subsection, we consider taking the mixture of two exponential kernels.

There are two kinds of mixing methods. The first one is taking the weighted average of two kernels, which maintains the positive definite property by the following fact.

Fact 6.3. If $k_i : \mathcal{X} \times \mathcal{X} \rightarrow \mathbb{C} (i = 1, 2, \dots)$ are strictly positive definite kernels, then the kernel $ak_1 + bk_2$ for $a, b \geq 0, ab > 0$, is also strictly positive definite.

The other mixing method is concatenation, which splits the input vectors into two parts, where the first part uses the first kernel, and the second part uses the second kernel. It is also easy to see that the concatenation of two strictly positive definite kernels is still strictly positive definite. We list the two types of kernel mixtures below.

Simple Sum Kernel:

$$K(x_i, x_j) \triangleq \exp(-\|f(\mathbf{x}_i) - f(\mathbf{x}_j)\|_2^2 / \tau_2) + \exp(-\|f(\mathbf{x}_i) - f(\mathbf{x}_j)\|_2^1 / \tau_1)$$

Concatenation Sum Kernel:

$$K(x_i, x_j) \triangleq \exp(-\|f(\mathbf{x}_i)[0 : n] - f(\mathbf{x}_j)[0 : n]\|_2^2 / \tau_2) + \exp(-\|f(\mathbf{x}_i)[n : 2n] - f(\mathbf{x}_j)[n : 2n]\|_2^1 / \tau_1)$$

7 Experiments

Method	CIFAR-10	
	200 epochs	400 epochs
SimCLR (repro.)	88.13	90.59
Laplacian Kernel	89.31	91.05
$\gamma = 0.5$ Exponential Kernel	89.00	91.23
Simple Sum Kernel	89.80	91.76
Concatenation Sum Kernel	89.89	91.28

Table 1: Results on CIFAR-10 dataset

Method	CIFAR-100	
	200 epochs	400 epochs
SimCLR (repro.)	62.67	66.23
Laplacian Kernel	63.17	66.06
$\gamma = 0.5$ Exponential Kernel	63.47	65.71
Simple Sum Kernel	66.73	68.62
Concatenation Sum Kernel	66.09	68.53

Table 2: Results on CIFAR-100 dataset

In our experiments, we reproduce the baseline algorithm SimCLR (Chen et al., 2020a), and replace SimCLR’s Gaussian kernel with other kernels, then test against SimCLR on different benchmark vision datasets.

Method	TinyImageNet	
	200 epochs	400 epochs
SimCLR (repro.)	34.03	37.86
Laplacian Kernel	35.92	38.76
$\gamma = 0.5$ Exponential Kernel	34.21	38.70
Simple Sum Kernel	36.60	39.38
Concatenation Sum Kernel	35.92	38.76

Table 3: Results on TinyImageNet dataset

CIFAR-10 and CIFAR-100 CIFAR-10 (Krizhevsky et al., 2009) and CIFAR-100 (Krizhevsky et al., 2009) are popular classical image classification datasets. Both CIFAR-10 and CIFAR-100 contain in total 60k 32×32 labeled images of different classes, which 50k for training and 10k for test. CIFAR-10 is similar to CIFAR-100, except there are 10 different classes in CIFAR-10, and 100 classes in CIFAR-100.

TinyImageNet TinyImageNet (Le & Yang, 2015) is a subset of ImageNet (Russakovsky et al., 2015). There are 200 different object classes in TinyImageNet, and 500 training images, 50 validation images, and 50 test images for each class. All the images in TinyImageNet are colored and labeled images with a size of 64×64 .

For each algorithm, we first train an encoder f on the training dataset, to minimize the empirical loss function generated by the kernel. Then following the standard linear evaluation protocol, we freeze the encoder f and train a supervised linear classifier, which takes the output representation of f as input. More experimental details can be found in Appendix B.

Experimental Results We summarize our empirical results on different benchmark datasets in Table 1, 2, and 3. It is clear that we have achieved better performance than SimCLR in all three benchmark datasets, and the Simple Sum Kernel reaches the best average performance.

8 Conclusion

In this paper, we take the probabilistic perspective of contrastive learning, and prove that it is essentially running spectral clustering on the predefined similarity graph. Extending this result to multi-modal learning, we show that CLIP is also doing the generalized spectral clustering on the pair graph. Based on the maximum entropy principle and other useful properties, we propose to use the mixtures of exponential kernels to replace the Gaussian kernel, which have achieved better performance empirically.

References

- Becker, S. and Hinton, G. E. Self-organizing neural network that discovers surfaces in random-dot stereograms. *Nature*, 355(6356):161–163, 1992.
- Chen, L. and Xu, S. Deep neural tangent kernel and laplace kernel have the same rkhs. *arXiv preprint arXiv:2009.10683*, 2020.
- Chen, T., Kornblith, S., Norouzi, M., and Hinton, G. A simple framework for contrastive learning of visual representations. In *International conference on machine learning*, pp. 1597–1607. PMLR, 2020a.
- Chen, X., Fan, H., Girshick, R., and He, K. Improved baselines with momentum contrastive learning. GitHub repository <https://github.com/facebookresearch/moco/tree/78b69cafae80bc74cd1a89ac3fb365dc20d157d3>, 2020b.
- Cui, J., Zhong, Z., Liu, S., Yu, B., and Jia, J. Parametric contrastive learning. In *Proceedings of the IEEE/CVF international conference on computer vision*, pp. 715–724, 2021.
- Hadsell, R., Chopra, S., and LeCun, Y. Dimensionality reduction by learning an invariant mapping. In *2006 IEEE Computer Society Conference on Computer Vision and Pattern Recognition (CVPR'06)*, volume 2, pp. 1735–1742. IEEE, 2006.
- HaoChen, J. Z., Wei, C., Gaidon, A., and Ma, T. Provable guarantees for self-supervised deep learning with spectral contrastive loss. *Advances in Neural Information Processing Systems*, 34: 5000–5011, 2021.
- Hassani, K. and Khasahmadi, A. H. Contrastive multi-view representation learning on graphs. In *International Conference on Machine Learning*, pp. 4116–4126. PMLR, 2020.
- He, K., Zhang, X., Ren, S., and Sun, J. Deep residual learning for image recognition. In *Proceedings of the IEEE conference on computer vision and pattern recognition*, pp. 770–778, 2016.
- He, K., Fan, H., Wu, Y., Xie, S., and Girshick, R. Momentum contrast for unsupervised visual representation learning. *arXiv preprint arXiv:1911.05722*, 2019.
- Hu, T., Liu, Z., Zhou, F., Wang, W., and Huang, W. Your contrastive learning is secretly doing stochastic neighbor embedding. *arXiv preprint arXiv:2205.14814*, 2022.
- Ioffe, S. and Szegedy, C. Batch normalization: Accelerating deep network training by reducing internal covariate shift. In *International Conference on Machine Learning*, pp. 448–456, 2015.
- Kalantidis, Y., Sariyildiz, M. B., Pion, N., Weinzaepfel, P., and Larlus, D. Hard negative mixing for contrastive learning. *Advances in Neural Information Processing Systems*, 33:21798–21809, 2020.
- Krizhevsky, A., Hinton, G., et al. Learning multiple layers of features from tiny images. 2009.
- Le, Y. and Yang, X. Tiny imagenet visual recognition challenge. *CS 231N*, 7(7):3, 2015.
- Li, L., Jamieson, K., Rostamizadeh, A., Gonina, E., Hardt, M., Recht, B., and Talwalkar, A. Massively parallel hyperparameter tuning. *arXiv preprint arXiv:1810.05934*, 5, 2018.
- Liaw, R., Liang, E., Nishihara, R., Moritz, P., Gonzalez, J. E., and Stoica, I. Tune: A research platform for distributed model selection and training. *arXiv preprint arXiv:1807.05118*, 2018.
- Lightning-AI. Pytorch-lightning, December 2022. URL <https://github.com/Lightning-AI/lightning/releases/tag/1.8.6>.
- Nair, V. and Hinton, G. E. Rectified linear units improve restricted boltzmann machines. In *Icmi*, 2010.
- Oord, A. v. d., Li, Y., and Vinyals, O. Representation learning with contrastive predictive coding. *arXiv preprint arXiv:1807.03748*, 2018.

- Radford, A., Kim, J. W., Hallacy, C., Ramesh, A., Goh, G., Agarwal, S., Sastry, G., Askell, A., Mishkin, P., Clark, J., et al. Learning transferable visual models from natural language supervision. In *International Conference on Machine Learning*, pp. 8748–8763. PMLR, 2021.
- Russakovsky, O., Deng, J., Su, H., Krause, J., Satheesh, S., Ma, S., Huang, Z., Karpathy, A., Khosla, A., Bernstein, M., et al. Imagenet large scale visual recognition challenge. *International journal of computer vision*, 115(3):211–252, 2015.
- Tian, Y. Understanding deep contrastive learning via coordinate-wise optimization. In *Advances in Neural Information Processing Systems*, 2022.
- Tian, Y., Sun, C., Poole, B., Krishnan, D., Schmid, C., and Isola, P. What makes for good views for contrastive learning? *Advances in Neural Information Processing Systems*, 33:6827–6839, 2020.
- Van Assel, H., Espinasse, T., Chiquet, J., and Picard, F. A probabilistic graph coupling view of dimension reduction. *Advances in Neural Information Processing Systems*, 2022.
- Wang, T. and Isola, P. Understanding contrastive representation learning through alignment and uniformity on the hypersphere. In *International Conference on Machine Learning*, pp. 9929–9939. PMLR, 2020.
- You, Y., Gitman, I., and Ginsburg, B. Scaling sgd batch size to 32k for imagenet training. *arXiv preprint arXiv:1708.03888*, 6(12):6, 2017.
- You, Y., Chen, T., Sui, Y., Chen, T., Wang, Z., and Shen, Y. Graph contrastive learning with augmentations. *Advances in Neural Information Processing Systems*, 33:5812–5823, 2020.

Algorithm 1 Augmented CLIP

Input: $\bar{\pi}_{A,B}$
repeat
 For every object a_i , sample its neighbor b'_i from $\bar{\pi}_{A,B}$.
 For every object b_i , sample its neighbor a'_i from $\bar{\pi}_{A,B}$.
 Train f once on $\{(a_i, b'_i)_{i=1}^{n_A}, (a'_i, b_i)_{i=1}^{n_B}\}$ with loss (1).
until f Converges

Algorithm 2 Multi-modal contrastive learning

Input: π^*
repeat
 For every object X_i , sample its neighbor X'_i (either in A or B) from π^* .
 Train f once on $\{(X_i, X'_i)\}_{i=1}^n$ with loss (1).
until f Converges

A Augmented CLIP

Can we modify CLIP so that it can produce semantically meaningful spectral clustering results, rather than depending on empirically verified network structures? This is possible if we have the data augmentation prior knowledge for both modalities. Formally, we define the augmented pair graph with the prior knowledge as follows.

Definition A.1 (Augmented pair graph). Given two similarity graphs $\pi_A \in \mathbb{R}_+^{n_A \times n_A}$, $\pi_B \in \mathbb{R}_+^{n_B \times n_B}$ representing the similarities in A and B respectively, we augment each edge $E_i = (a_i, b_i, p_i)$ in $\pi_{A,B} \in \mathbb{R}_+^{(n_A+n_B) \times (n_A+n_B)}$ to be $\bar{E}_i \triangleq \{(\bar{a}_i, \bar{b}_i, p_i \cdot \pi_A(a_i, \bar{a}_i) \cdot \pi_B(b_i, \bar{b}_i)) \mid \bar{a}_i \sim \pi_A(a_i), \bar{b}_i \sim \pi_B(b_i)\}$, where $\pi_A(a_i)$ denotes the probability distribution of augmenting a_i in A , $\pi_A(a_i, \bar{a}_i)$ denotes the sampling probability of pick \bar{a}_i given a_i . $\pi_B(b_i)$ and $\pi_B(b_i, \bar{b}_i)$ are defined similarly. $\bar{\pi}_{A,B}$ is the combination of all \bar{E}_i .

After augmentation, each pair will connect two groups of objects with similar semantic meanings, instead of just two isolated objects. Running CLIP on the augmented pair graph, we immediately get the following corollary.

Corollary A.2 (Augmented CLIP). *Denote the pair graph as $\bar{\pi}_{A,B}$, then Algorithm 1 is equivalent to running the generalized spectral clustering on $\bar{\pi}_{A,B}$.*

Algorithm 1 runs spectral clustering on the bipartite graph $\bar{\pi}_{A,B}$, and contrastive learning runs spectral clustering on π_A and π_B . Can we combine these algorithms to run spectral clustering on all the graphs glued together? This naturally leads to the following definition.

Definition A.3 (Multi-modal similarity graph). Given two similarity graphs π_A, π_B , and an augmented pair graph $\bar{\pi}_{A,B}$, we glue all these graphs together to get the multi-modal similarity graph π^* , with adjusted probabilities.

Here adjusted probability means we scale all the probabilities in π_A and π_B by say, 0.3, and the probabilities in $\bar{\pi}_{A,B}$ by 0.4, so that each row of π^* is still a valid probability distribution. The scaling factors can be set as a hyperparameter empirically.

π^* is a hybrid graph with inter- and intra-modal edges, which is a different setting from CLIP or standard contrastive learning. However, if we treat the two encoders as a single function f that can encode the objects from both A and B , we can still run the InfoNCE loss on the graph, see Algorithm 2. We have the following corollary, which can be naturally generalized to more than two modalities.

Corollary A.4 (Multi-modal contrastive learning). *Denote the multi-modal similarity graph as π^* , then Algorithm 2 is equivalent to running the generalized spectral clustering on π^* .*

B Experiment Details

Pseudo-Code. Algorithm 3 shows the pseudo-code for our empirical training procedure.

Algorithm 3 Training Procedure

Require: trainable encoder network f , batch size N , augmentation strategy aug , loss function L with hyperparameters $args$

- 1: **for** sampled minibatch $\{x_i\}_{i=1}^N$ **do**
- 2: **for all** $i \in \{1, \dots, N\}$ **do**
- 3: draw two augmentations $t_i = aug(x_i)$, $t'_i = aug(x_i)$
- 4: $z_i = f(t_i)$, $z'_i = f(t'_i)$
- 5: **end for**
- 6: compute loss $\mathcal{L} = L(N, z, z', args)$
- 7: update encoder network f to minimize \mathcal{L}
- 8: **end for**
- 9: **Return** encoder network f

We also provide the pseudo-code of our core loss function used in training procedure in Algorithm 4. The pseudo-code is almost the same with SimCLR’s loss function, except we have an extra parameter γ .

Algorithm 4 Core loss function \mathcal{C}

Require: batch size N , two encoded minibatches z_1, z_2, γ , temperature τ

- 1: $z = concat(z_1, z_2)$
- 2: **for** $i \in \{1, \dots, 2N\}, j \in \{1, \dots, 2N\}$ **do**
- 3: $s_{i,j} = \|z_i - z_j\|_2^\gamma$
- 4: **end for**
- 5: **define** $l(i, j)$ **as** $l(i, j) = -\log \frac{\exp(s_{i,j}/\tau)}{\sum_{k=1}^{2N} \mathbf{1}_{[k \neq i]} \exp(s_{i,j}/\tau)}$
- 6: **Return** $\frac{1}{2N} \sum_{k=1}^N [l(i, i + N) + l(i + N, i)]$

With the help of core loss function \mathcal{C} , we can define all kernel loss function used for our experiments in Table 4. Here for all $z_i \in z$ with even dimensions n , we define $z_{L_i} = z_i[0 : n/2]$ and $z_{R_i} = z_i[n/2 : n]$

Kernel	Loss function
Laplacian	$\mathcal{C}(N, z, z', \gamma = 1, \tau)$
Sum	$\lambda * \mathcal{C}(N, z, z', \gamma = 1, \tau_1) + (1 - \lambda) * \mathcal{C}(N, z, z', \gamma = 2, \tau_2)$
Concatenation Sum	$\lambda * \mathcal{C}(N, z_L, z'_L, \gamma = 1, \tau_1) + (1 - \lambda) * \mathcal{C}(N, z_R, z'_R, \gamma = 2, \tau_2)$
$\gamma = 0.5$	$\mathcal{C}(N, z, z', \gamma = 0.5, \tau)$

Table 4: Definition of kernel loss functions in our experiments

Baselines. We reproduce SimCLR algorithm based on PyTorch LightningLightning-AI (2022).

Encoder Details. The encoder f consists of a backbone network and a projection network. We use ResNet50He et al. (2016) as the backbone, and a 2-layer MLP (linked by a batch normalization Ioffe & Szegedy (2015) layer and a ReLU Nair & Hinton (2010) layer) with hidden dimensions 2048 and output dimensions 128(or 256 in concatenation kernel case).

Encoder Hyperparameter Tuning. For each encoder training case, we sample 500 hyperparameter groups randomly (sample detail is shown in Table 5), and train these samples simultaneously using Ray TuneLiaw et al. (2018), with ASHA scheduler Li et al. (2018). Finally, the hyperparameter group that maximizes the online validation accuracy (integrated in PyTorch Lightning) in 5000 validation steps is chosen to be used in this encoder training case.

Encoder Training. We train each encoder using LARS optimizer You et al. (2017), LambdaLR Scheduler in PyTorch, momentum 0.9, weight decay 10^{-6} , batch size 256 together with above hyperparameters for 800 epochs, in one A-100 GPU.

Image Transformation. The image transformation strategy, includes argumentation, is the same as the default transformation strategy given by PyTorch Lightning

Hyperparameter	Sample Range	Sample Strategy
start learning rate	$10^{-2}, 10$	log uniform
λ	$[0, 1]$	uniform
τ, τ_1, τ_2	$[0, 1]$	log uniform

Table 5: Hyperparameters sample strategy

Linear Evaluation. The linear head is trained using SGD optimizer with cosine learning rate scheduler, batch size 64, and weight decay 10^{-6} for 100 epochs, and the learning rates starts at 0.3, ends at 0.